Article:
McGhie, A, Marquina, C, O'Grady, Kevin Dermot orcid.org/0000-0002-4837-3709 et al. (1 more author) (2017) Measurement of the distribution of anisotropy constants in magnetic nanoparticles for hyperthermia applications. Journal of Physics D: Applied Physics. 455003. ISSN 1361-6463

Measurement of the distribution of anisotropy constants in magnetic nanoparticles for hyperthermia applications

A. A. McGhie,[1] C. Marquina,[2,3] K O'Grady[1,4] and G. Vallejo-Fernandez[1]

[1]*Department of Physics, University of York, York, YO10 5DD, UK*

[2] *Departamento de Física de la Materia Condensada, Universidad de Zaragoza, 50009-Zaragoza, Spain.*

[3]*Instituto de Ciencia de Materiales de Aragón (ICMA); Consejo Superior de Investigaciones Científicas (CSIC)-Universidad de Zaragoza, 50009-Zaragoza, Spain.*

[4]*Liquids Research Ltd, Unit 3B Mentec, Deiniol Road, Bangor, Gwynedd, LL57 2UP, UK*

Abstract

In this work we have applied theoretical calculations to new experimental measurements of the effect of the anisotropy distribution in magnetite nanoparticles which in turn controls hysteresis heating for hyperthermia applications. Good agreement between theory and experiment is reported where the theoretical calculation is based upon the detailed measurement of the particle elongation generally observed in the nanoparticles. The elongation has been measured from studies via transmission electron microscopy (TEM). We find that particle elongation is responsible for the anisotropy dispersion which can be obtained by analysis and fitting to a measurement of the temperature decay of remanence. A median value of the anisotropy constant of $1.5x10^5$erg/cc was obtained. A very wide distribution of anisotropy constants is present with a Gaussian standard deviation of $1.5x10^5$erg/cc. From our measurements, deviations in the value of the saturation magnetisation from particle to particle are most likely the main factor giving rise to this large distribution with 33% arising from the error in the measured elongation. The lower limit to the anisotropy constant of the nanoparticles is determined by the magnetocrystalline anisotropy of the material, $1.1x10^5$erg/cc for magnetite which was studied in this work.

1. Introduction

The general treatment for benign brain tumours and most forms of malignant cancer is via surgery followed by chemotherapy or radiotherapy both of which cause significant side effects. In particular the treatment of inoperable benign brain tumours is generally via positron irradiation which almost invariably leads to collateral damage of healthy tissue which causes severe and, sometimes, terminal side effects due to hardening of the arteries in the brain [1]. For other growths such as prostate cancer any treatment regime to reduce the size of the gland is generally very unpleasant leading to late reporting of the illness. Magnetic hyperthermia has been studied actively for about the last 15 years and is now at the stage where human trials have begun and successful outcomes have been reported [2]. A recent comprehensive review on this topic can be found in [3]. One key difficulty in developing a comprehensive theory arises from the fact that the measured heat output of a sample of magnetic nanoparticles depends upon the measurement technique used [4]. The synthesis method used also plays a role [5] as well as the concentration level and hydrodynamic properties of the fluid [6]. Reference to the literature shows that even for systems containing very similar particles different heating rates are reported [7,8]. This means that the development of a clear dosimetric strategy for use by clinicians is not yet available. There is an urgent need to develop a clear and experimentally validated model which predicts the magnitude of the effect thereby allowing for the definition of the most appropriate particle size, field amplitude and frequency to obtain a given therapeutic outcome.

In a recent work we have shown both theoretically and experimentally that there are three distinct processes by which heat can be generated in colloids of nanoparticles. At frequencies used in hyperthermia experiments susceptibility losses are negligible with heat generation being dominated by viscous heating and hysteresis losses [9]. For magnetic hyperthermia the frequency used is generally of the order of 100 kHz. In the case of hysteresis heating the power generated (P_{hys}) is proportional to the frequency of the AC field multiplied by the area of the hysteresis loop. However it is only the irreversible switching of the magnetisation that will contribute to the heating effect. The hysteresis for each particle size can be represented by a so called hysteron as defined by the well known Preisach

model [10]. This gives each particle a remanence equal to $0.5m_s$ where m_s is the moment of the particle. Therefore P_{hys} can be written as

$$P_{hys} = \frac{2M_s}{\rho} f \int_{V_p(0)}^{V_p(H)} H_c(V) f(V) dV \quad (1)$$

where M_s is the saturation magnetisation of the material, f is the frequency of measurement, ρ is the density of the material, $H_c(V)$ is the coercivity of a particle of volume V and $f(V)dV$ is the distribution of particles volumes within the system. The two limits in the integral Eq. 1 represent the critical volume for superparamagnetic behaviour ($V_p(0)$) and the maximum particle volume that can be switched given the amplitude (H) of the AC field ($V_p(H)$).

Following the publication of our original work it has been brought to our attention that not only will the particle volume distribution determine the heating mechanism for magnetic hyperthermia applications but also the distribution of the anisotropy constants, (g(K)), will also affect the critical volumes highlighted in Eq. 1. For any in-vivo application of hysteresis heating only the ferrimagnetic iron oxides magnetite and maghemite are approved for use by the appropriate regulatory medical authorities. These oxides generally have a low magnetocrystalline anisotropy and a dominant shape anisotropy given by

$$K_s = \frac{1}{2}(N_a - N_c)M_s^2 \quad (2)$$

where N_a and N_c are the demagnetising factors which for a prolate spheroid are given by

$$N_c = \frac{4\pi}{r^2 - 1}\left[\frac{r}{\sqrt{r^2 - 1}} \ln(r + \sqrt{r^2 - 1}) - 1\right] \quad (3)$$

$$N_a = \frac{4\pi - N_c}{2} \quad (4)$$

where r is the aspect ratio of the particles. The value of the magnetocrystalline anisotropy for magnetite is of the order of 1.1×10^5 erg/cc [11]. However for the case of the magnetocrystalline anisotropy of cubic materials such as the iron oxides, the energy barrier to reversal is KV/4, not KV, as for the uniaxial case. Hence the effective anisotropy constant to switching for the crystalline anisotropy is actually 0.25×10^5 erg/cc. Using a value of M_s of 420 emu/cc, shape anisotropy becomes dominant for $r > 1.05$ (5%

elongation) [12]. It is well known that magnetite particles will oxidise in an aqueous medium to form maghemite resulting in a value of M_s generally lower than that of the bulk (480 emu/cc). Hence, the lower value used.

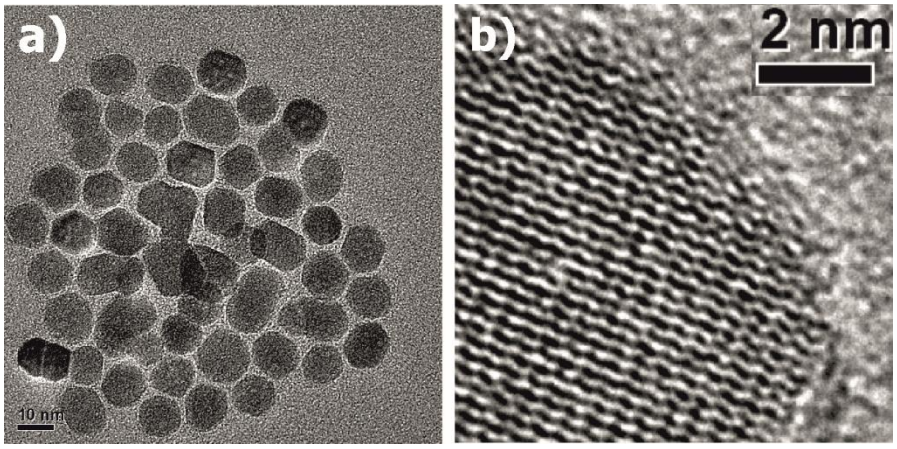

Figure 1. (a) Typical TEM image of the sample used in this work and (b) high resolution TEM image showing the lack of crystallisation at the surface.

Figure 1(a) shows a TEM image for the same sample studied in this work. A casual inspection of the particles in this image indicates that almost all particles have an aspect ratio greater than 1.05 and in several cases particle elongations greater than 2 can be observed. This will give rise to a shape anisotropy constant more than an order of magnitude greater than the crystalline term and the variation in particle shape will thereby give rise to a significant distribution for the anisotropy constant given by g(K). Eq. 1 assumes a uniform value of K but the data provided above indicates that this is very much an approximation. In a paper subsequent to our original work [12] we presented a theoretical analysis where a distribution of K was assumed. This results in the critical parameters $V_p(0)$ and $V_p(H)$ not being fixed. In consequence, particles of a given size might not be blocked whilst other particles of the same size might be superparamagnetic giving rise to a critical energy barrier ΔE_c. We have shown that this now gives rise to a revised expression for the hysteresis heating power P_{hys} [12]

$$P_{hys} = \frac{2M_s}{\rho} f \int_0^\infty \int_0^\infty H_c(V) f(V) g(K) \delta(K,V) dK dV \qquad (5)$$

The parameter δ(K,V) is a δ function equal to 1 when the particles are blocked and can be switched and zero otherwise.

The distribution of particle sizes is generally lognormal of the form

$$f(D)dD = \frac{1}{\sqrt{2\pi}\sigma_{\ln D}D}\exp\left[-\frac{\ln\left(D/D_m\right)^2}{2\sigma_{\ln D}^2}\right]dD \quad (6)$$

However as we will show in this work the distribution of the anisotropy constants is Gaussian and is given by

$$g(K)dK = \frac{1}{\sqrt{2\pi}\sigma_K}exp\left[-\frac{(K-K_m)^2}{2\sigma_K^2}\right]dK \quad (7)$$

where σ_{lnD} is the standard deviation of ln(D) and σ_K is the standard deviation of the distribution of anisotropy constants. The mean values of the distribution are D_m and K_m.

2. Methods

The measurement of the anisotropy constant of any material and particularly magnetic nanoparticle systems is extremely challenging. A long standing technique originally due to Gittleman [13] and subsequently applied by ourselves to a solidified ferrofluid [14] allows the mean value of the anisotropy constant K_m to be determined if the median diameter of the particle size distribution is known to high accuracy. This is achieved via a measurement of the temperature decay of remanence starting from low temperatures where the sample, whether a colloid or not, will be in the frozen state and consist of blocked particles. When the sample is frozen in zero field a remanence to saturation ratio M_r/M_s=0.5 is expected following standard Stoner Wohlfarth theory for a system of blocked particles. The remanence at any temperature is given by

$$\frac{M_r(T)}{M_s} = 0.5\left(1 - \int_0^{V_P(T)} f(V)dV\right) \quad (8)$$

where $V_p(T)$ is the critical size for superparamagnetic behaviour at a given temperature T. As the temperature increases the remanence ratio falls as an increasing fraction of the particles in the distribution, i.e. the smaller particles, become superparamagnetic. At the point where the remanence has reached 50% of its initial value, exactly half the volume of magnetic material in the colloid has

become superparamagnetic and the median value of the anisotropy constant K_m can be obtained. However, this technique is only valid when a narrow distribution of anisotropy constants is present. In our case and in most experimental cases, the distribution of particle sizes and elongations are not independent. As result, the temperature at which the remanence reaches half of its maximum value determines the median value of the energy barrier to reversal $\Delta E_m = \langle KV \rangle$ rather than K_m. Hence, Eq. 8 has to be rewritten as

$$\frac{M_r(T)}{M_s} = 0.5\left(1 - \int_0^\infty \int_0^\infty f(V)g(K)\delta(K,V)dVdK\right) \tag{9}$$

where the temperature dependence is included in the δ(K,V) function. In this work we have undertaken high resolution measurements of the temperature decay of remanence and used computer graphic techniques to measure the distribution of particle elongations so that the physical distribution of shape anisotropy constants can be obtained via Eq. 2.

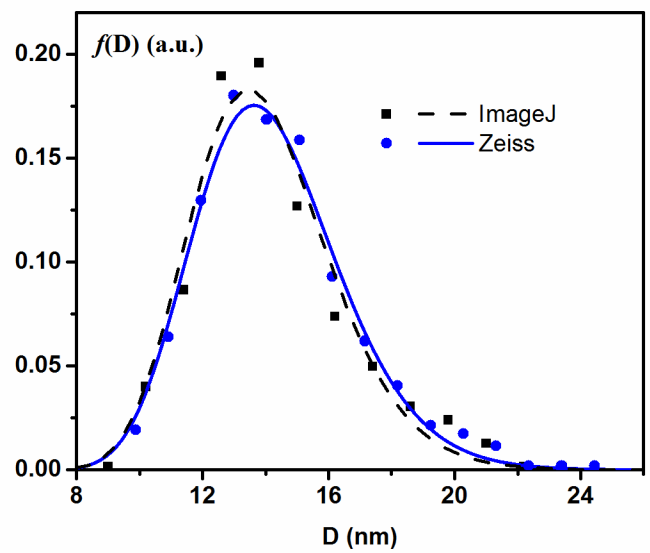

Figure 2. Particle size distribution measured using a Zeiss particle size analyser and ImageJ.

3. Results

The medical requirements for particles to be used in magnetic hyperthermia generally means that they must be made via an aqueous process. The sample studied in this work was made by a variation of the well known co-precipitation process [15] in which salts of Fe^{2+} and Fe^{3+} are treated with an alkali

resulting in the precipitation of magnetite. This process generally produces a wide distribution of particle size but careful control of the growth conditions allows for a narrow distribution of particle sizes to be obtained. The materials were prepared by Liquids Research Ltd using this process which is known as the Controlled Growth Process with the products being designated CGP particles with the brand name HyperMAG® [16]. The quality of the resulting particles and the width of the size distribution can be seen in Figs. 1a and 2, respectively. From these figures it is clear that most of the particles are elongated at least to a degree greater than the 5% elongation required to give dominant shape anisotropy. Furthermore careful examination of figure 1(a) shows that some of the particles have clearly fused together producing dimers or even trimers.

The dispersion of magnetic nanoparticles in water generally results in a degree of aggregation. Hence for this basic scientific study the particles have been dispersed in a simple C_{22} straight chain isoparaffin oil (Isopar V) using oleic acid. The concentration of nanoparticles in the dispersion was kept at a level such that the total concentration of Fe in the colloid was 5mg/ml of solution as this is the limit given by the FDA use in humans. The resulting magnetic concentration of the colloids was of the order of 5 Gauss. Colloids with this low concentration of magnetic nanoparticles have advantages for magnetic measurements. For bulk magnetic measurements the resulting demagnetising field is very low for all magnetisation values if sample holders with an axial ratio of 2:1 are used. Hence there is no need for a correction to the magnetic measurements to be applied. Secondly it has been shown by computational modelling that well dispersed colloids at this concentration do not suffer from any significant effect from the dipolar interactions between the individual particles [17]. However where significant aggregation of the particles occurs a local concentration far higher than 5 vol % can result leading to significant effects from dipole-dipole interactions. This possibility was prevented by subjecting the colloids to a magnetic separation process to remove any aggregated material.

The particle size distribution was measured from TEM images such as that shown in figure 1(a). The images were obtained using a JEOL 2011 TEM with an accelerating voltage of 200 keV having a resolution of 2Å. Multiple images from different regions of the TEM grid were obtained so that at least

500 particles could be measured not only to define the median diameter D_m but to give an accurate value for the standard deviation of the distribution σ_{lnD}. Particle size measurements were obtained initially using a Zeiss particle size analyser which consists of a light box with a variable aperture. The resulting circular beam of light was used to obtain the particle diameter via an equivalent circle method. Where particles were significantly elongated, human judgment was used to obtain the equivalent circle. The resulting lognormal distribution function was calculated from the experimental data by calculating the Gaussian distribution of lnD rather than fitting a distribution to the measurements.

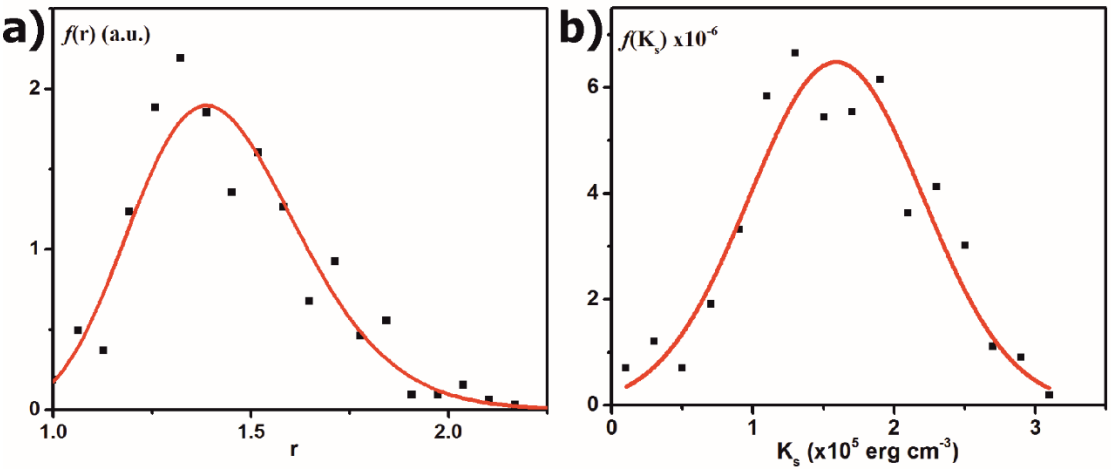

Figure 3. (a) Distribution of aspect ratios and (b) anisotropy constants, where a magnetic dead layer has been taken into account.

Measurements of the particle elongation were obtained using the software package ImageJ [18]. The particle size was recorded simultaneously so that the possible correlation between particle size and shape could be determined. The number of pixels forming the particle were converted into an area and from this value the particle size was calculated assuming an equivalent circle method. To remove the influence of human error on the measurements, the images of the particles were magnified and converted to a black and white scale. The elongation itself was then measured again by using a pixelated image of each particle and the elongation determined from the ratio of the maximum number of pixels in a given particle to the minimum number in a direction approximately orthogonal to the long axis. Again more than 500 particles were measured. In a similar manner to the determination of the particle size distribution, the anisotropy constant distribution was obtained via Eq. 2 and characterised by a

median value K_m and a standard deviation σ_K. Figure 3 shows the particle size distributions obtained using both the Zeiss system and ImageJ. From these two fits the median particle size D_m was 14.3 and 14.0 nm, respectively. There is also excellent agreement in the measured value of σ_{lnD} obtained using both techniques, 0.16 and 0.17, respectively. We believe this in an indication of the quality of our particle size distribution measurement.

Figure 3(a) shows the distribution of particle elongations in our system. For our calculation of the aspect ratio, r, we have assumed that the two outer atomic layers in each particle are magnetically dead. This is consistent with the remanence measurements shown later in this work. The distribution appears to be lognormal with a fit shown. Eq. 2 can be used to convert the data in figure 3(a) into a distribution of anisotropy constants. This is shown in Figure 3(b). The distribution of anisotropy constants appears to be Gaussian with a median value K_m of 1.5×10^5 erg/cc and a standard deviation $\sigma_K = 0.5 \times 10^5$ erg/cc. Note that the magnetic dead layers will also have an effect of the effective median particle size. If two atomic layers are removed from the outer layers of each particle, the average size is reduced from 14.1 nm to 12.9 nm, assuming that each atom results in a reduction of the effective particle size of 0.3 nm.

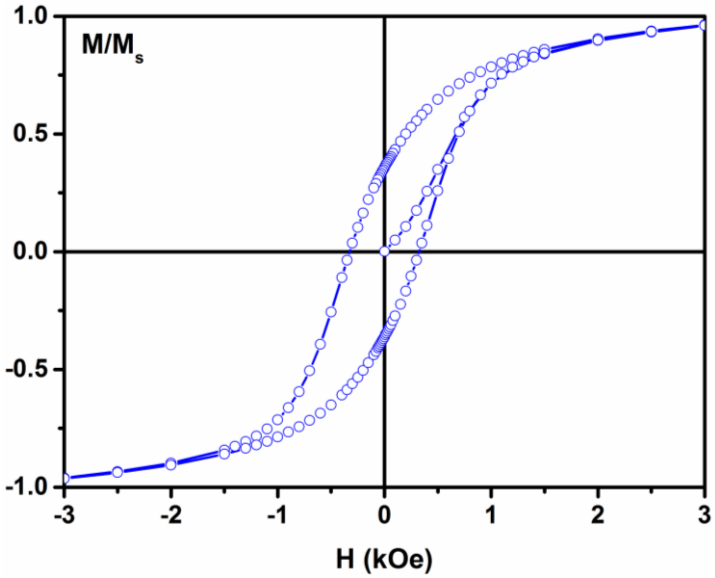

Figure 4. M-H loop for this sample showing the major hysteresis loop for the nanoparticles.

The hysteresis loops for our sample were measured using a SQUID magnetometer fitted with a continuous flow cryostat allowing temperatures from 1.8 K to 350 K to be obtained. The sample was cooled in zero field to 1.8 K and saturated in a maximum field of 50 kOe. Figure 4 shows the hysteresis loops for the sample measured at 1.8 K. The coercivity of the sample is 325Oe. From the Stoner-Wohlfarth theory, the coercivity of a system of non-interacting magnetic nanoparticles with randomly oriented easy axes is given by $0.96K/M_s$ [19]. Using the measured value of K of $1.5x10^5$ erg/cc and M_s of 420 emu/cc, the expected value of the coercivity was 343 Oe which is in very good agreement with our magnetic measurement. From the closure point of the hysteresis loop at 2 kOe it is clear that a saturation field of 5 kOe is adequate to switch all the blocked particles in the sample even at this low temperature. Hence, for the temperature decay of remanence the sample was saturated in a field of 5 kOe. The field was then removed and the remanence measured after a waiting time of 100 seconds. The temperature was then increased in steps of 2-5 K and the remanence measured after re-saturating the sample. It can also be seen that the loop squareness is somewhat less than the value of 0.5 expected from the Stoner Wohlfarth model. This is a well known effect for measurements on dispersions of magnetic particles. It derives from the fact that the bonding of the surfactant at the particle surface leads to a partially magnetic dead layer due to the bonding between the carboxylic acid and the Fe^{2+}. However the Fe^{2+} irons are still paramagnetic thereby artificially increasing the measured value of M_s and preventing the hysteresis loop from fully saturating [20]. The saturation magnetisation of the core of the nanoparticles was then taken as being equal to $2M_r$ in accordance with the Stoner Wohlfarth theory. The presence of a magnetic dead layer, ~2 atoms thick, is evident in Figure 1(b). We have deemed that the point at which half the magnetic volume had become superparamagnetic was that at which the value of the remanence was equal to half that at 1.8 K.

Figure 5 shows the measurement of the temperature decay of remanence for this material. The 50% point in the temperature decay of remanence occurs at a temperature $T_B = (74\pm3)$ K. The raw data shows that the value of the remanence at 1.8 K is equal to ~$0.37M_s$. A 14.1 nm nanoparticle, assuming it is spherical for simplicity, has a volume of ~11750 nm^3. Assuming the magnetic dead layer is two atoms thick (6Å) the effective particle diameter is now 12.9 nm. The volume of a particle of such size is ~9000

nm^3, i.e. ~24% smaller than the equivalent 14.1 nm particle. Hence the remanence would be expected to be 24% smaller or $0.38M_s$ which is consistent with our VSM measurements.

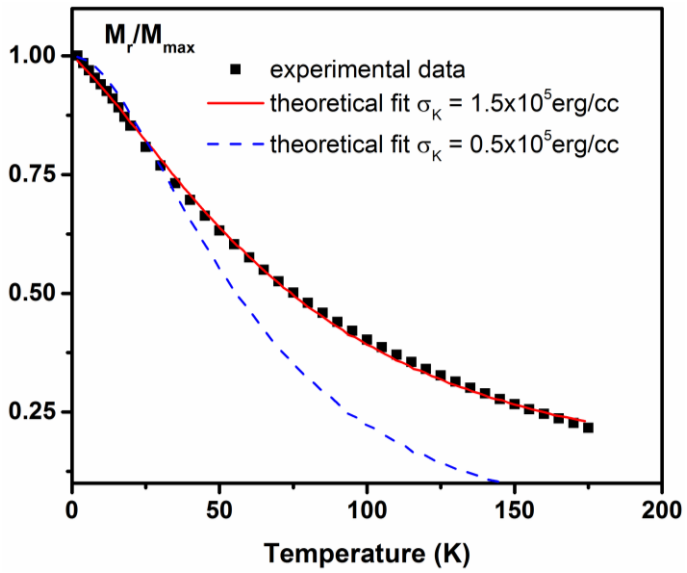

Figure 5. Temperature decay of remanence curve. The solid line shows the theoretical fit to the data from Eq. 9.

Using Eq. 9 it is now possible to fit a theoretical line to the data in figure 5 with the parameters required in Eq. 2 having been determined experimentally. However it is apparent from the TEM image in figure 1(a) that the distribution of particle elongations is not uniform with particle size. The presence of a number of dimers and trimers indicates that there is a particle size dependence of the elongation. Using the particle size/elongation data obtained using ImageJ (>500 individual measurements) we have compared the degree of elongation with the particle size as shown in figure 6. Whilst the relationship is not particularly monotonic the fitted line through the data (Pearson's r = 0.9259) indicates that some correction is required. The error bars in figure 6 correspond to the standard deviation arising from binning the raw data. For our calculations we have applied a linear correction so that larger particles were assumed to have a larger average elongation. The standard deviation of the elongation does not seem to depend on the particle size.

There are two calculated fits shown in figure 5. In both cases, the following fitting parameters were used: D_m = 12.9 nm, σ_{lnD} = 0.17, $K_m = 1.5x10^5$ erg/cc, M_s = 420 emu/cc and waiting time of 100 s.

The only difference in the fits is the standard deviation of the distribution of anisotropy constants. For the dashed line in figure 5(a) value of $\sigma_K = 0.5 \times 10^5$ erg/cc was used. This was the value calculated from the particle elongation measurements. As can be seen from figure 5, the quality of the fit is quite poor. The agreement between theory and experiment can be significantly improved by using a value of σ_K of 1.5×10^5 erg/cc. This corresponds to a 100% dispersion in the distribution of anisotropy constants although a lower limit of K of 1.1×10^5 erg/cc was used corresponding to the magnetocrystalline anisotropy constant for magnetite [11]. In order to understand the origin of this discrepancy we have to examine Eq. 2. The value of the shape anisotropy constant depends not only on a given particle's elongation but also on its saturation magnetisation. Moreover, K_s varies as the square of M_s so any deviation in M_s from particle to particle will have a significant effect on the distribution of anisotropies. The origin of this is likely to be the presence of both maghemite and magnetite phases of iron oxide within the sample. Other reasons for this broadening can be the faceting of the nanoparticles, presence of defects or, to a lesser extent, stress within the particles. For our sample it appears that 33% of the dispersion in K arises due to particle elongation effects with the remainder deriving from compositional and structural effects.

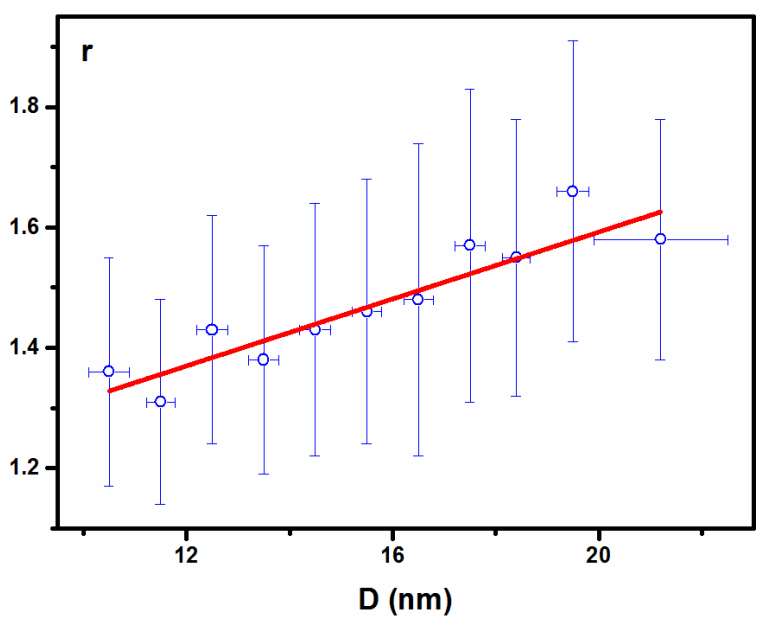

Figure 6. Particle size compared with particle elongation. Note that the error bars in the r axis is the standard deviation of many measurements.

Using Eq. 5 we have calculated the hysteresis heating that would be observed for a system characterised by the parameters used in the better fitting in figure 5 and compared it to the heating that would be expected in an equivalent system where K is uniform. For the calculations a field amplitude of 180 Oe and a frequency of 111.5 kHz were used while the density of magnetite was taken as 5.175 g/cm^3. When a distribution of anisotropy constants is present, the expected heat output was found to be 17.2 W/g_{Fe} while when K is uniform that value is expected to drop to 3.9 W/g_{Fe}, 77% lower. Although this calculation specifically applies to the sample studied in this work, it highlights the general need for characterising a given sample not only by its particle size distribution but also by its distribution of anisotropy constants. It explains why different studies in the literature using similar samples, i.e. same material and very similar particle size and measurement conditions give rise to very different heat outputs.

4. Conclusions

We have shown that a distribution of anisotropy constants is present in systems consisting of magnetic nanoparticles. The origin of this distribution is the elongated nature of the particles with the presence of different ferrimagnetic phases giving rise to a very broad distribution of anisotropy constants. Careful measurement of the particle size and shape distributions has allowed for the determination of the median value of the anisotropy constant for such systems. A temperature decay of remanence measurement has been used to determine the width of the distribution of anisotropy constants present in the system. This distribution needs to be taken into account when calculating the heating efficiency of a given system for magnetic hyperthermia applications.

Acknowledgements

The authors would like to acknowledge the use of Servicio General de Apoyo a la Investigación-SAI at Universidad de Zaragoza.

References

[1] D. M. Gujral, B. N. Shah, N. S. Chahal, R. Senior, K. J. Harrington, and C. M. Nutting, Clin. Onc. 26, 94 (2014).

[2] M. Johannsen, U. Gneveckow, L. Eckelt, A. Feussner, N. Waldöfner, R. Scholz, S. Deger, W. Wust, S. A. Loening, A. Jordan, Int. J. Hyperthermia **21** 637 (2005).

[3] Z. Hedayatnasab, F. Abnisa, W. M. Ashri and W. Daud, Materials and Design, 123 174 (2017).

[4] M. Coïsson, G. Barrera, F. Celegato, L. Martino, S. N. Kane, S. Raghuvanshi, F. Vinai, and P. Tiberto, Biochimica et Biophysica Acta 1861, 1545 (2017).

[5] S. Gyergyek, D. Makovec, M. Jagodič, M. Drofenik, K. Schenk, O. Jordan, J. Kovač, G. Dražič, and H. Hofmann, J. of Alloys and Compounds 694, 261 (2017).

[6] B. B. Lahiri, S. Ranoo, A. W. Zaibudeen, J. Philip, J. Magn. Magn. Mater. 441, 310 (2017).

[7] E. Natividad, M. Castro, and A. Mediano, Appl. Phys. Lett. 92, 093116 (2008).

[8] M. Ma, Y. Wu, J. Zhou, Y. Sun, Y. Zhang, and N. Gu, J. Magn. Magn. Mater. 268, 33 (2004).

[9] G. Vallejo-Fernandez, O. Whear, A. G. Roca, S. Hussain, J. Timmis, V. Patel, and K. O'Grady, J. Phys. D: Appl. Phys. 46 312001 (2013).

[10] F. Preisach Zeitschrift für Physik. 94, 277 (1935).

[11] B. D. Cullity, and C. D. Graham, Introduction to Magnetic Materials, (IEEE Press, Wiley, 2nd Edition, New Jersey) page 227 (2009).

[12] G. Vallejo-Fernandez and K. O'Grady, Appl. Phys. Lett. 103 142417 (2013).

[13] J. I. Gittleman, B. Abelas, and S. Bozowski, Phys. Rev. B 9, 2891 (1994).

[14] K. O'Grady, R. W. Chantrell, and J. Popplewell, IEEE Trans. Magn. 16 1077 (1980).

[15] S. E. Khalafalla, and G. W. Reimens, IEEE Trans. Magn. 16, 178 (1980).

[16] http://www.liquidsresearch.com/

[17] F. Burrows, C. Parker, R. F. L. Evans, Y. Hancock, O. Hovorka and R. W. Chantrell, J. Phys. D: Appl. Phys. 43, 474010 (2010).

[18] https://imagej.nih.gov/ij/

[19] F. E. Luborsky, J. Appl. Phys. **32** 171S (1961).

[20] R. H. Kodama, A. E. Berkowitz, E. J. McNiff Jr. and S. Foner, J. Appl. Phys. 81 5552 (1997).